Available online at www.sciencedirect.com
ScienceDirect
Biochimica et Biophysica Acta 1757 (2006) 1052–1063
BIOCHIMICA ET BIOPHYSICA ACTA
BBA
www.elsevier.com/locate/bbabio

Review

Transmembrane proton translocation by cytochrome *c* oxidase

Gisela Brändén [a], Robert B. Gennis [b,*], Peter Brzezinski [a,*]

[a] *Department of Biochemistry and Biophysics, The Arrhenius Laboratories for Natural Sciences, Stockholm University, SE-106 91 Stockholm, Sweden*
[b] *School of Chemical Sciences, University of Illinois, Urbana, IL, 1801, USA*

Received 6 April 2006; received in revised form 11 May 2006; accepted 12 May 2006
Available online 19 May 2006

Abstract

Respiratory heme-copper oxidases are integral membrane proteins that catalyze the reduction of molecular oxygen to water using electrons donated by either quinol (quinol oxidases) or cytochrome *c* (cytochrome *c* oxidases, C*c*Os). Even though the X-ray crystal structures of several heme-copper oxidases and results from functional studies have provided significant insights into the mechanisms of O_2-reduction and, electron and proton transfer, the design of the proton-pumping machinery is not known. Here, we summarize the current knowledge on the identity of the structural elements involved in proton transfer in C*c*O. Furthermore, we discuss the order and timing of electron-transfer reactions in C*c*O during O_2 reduction and how these reactions might be energetically coupled to proton pumping across the membrane.

Keywords: Cytochrome aa_3; Quinol oxidase; Electron transfer; Proton transfer; Electrochemical proton gradient

1. Introduction

The heme-copper oxidases are found in the inner mitochondrial membrane in eukaryotes or in the bacterial cytoplasmic membrane. In cytochrome *c* oxidase (C*c*O), the electrons are donated from the inter-membrane space (or periplasmic side in bacteria), while the protons are taken up from the inside of the membrane (mitochondrial matrix or the cytosol in bacteria). Therefore, the reaction catalyzed by the C*c*Os results in a charge separation across the membrane corresponding to movement of one positive charge across the membrane per electron transferred to O_2. In addition, in many respiratory oxidases, for each electron transferred to oxygen, an average of one proton is pumped through the enzyme ([1], see also [2]) such that the overall reaction catalyzed by C*c*O is:

$$4\mathrm{cyt}.c^{2+}_{\mathrm{out}} + \mathrm{O_2} + 4\mathrm{H}^{+}_{(\mathrm{s})\mathrm{in}} + 4\mathrm{H}^{+}_{(\mathrm{p})\mathrm{in}} \rightarrow 4\mathrm{cyt}.c^{3+}_{\mathrm{out}} + 2\mathrm{H_2O} + 4\mathrm{H}^{+}_{(\mathrm{p})\mathrm{out}} \quad (1)$$

where the subscripts "s" and "p" denote substrate (used for water formation) and pumped protons, respectively, and "in" and "out" denote the inner mitochondrial matrix (or the cytosol in bacteria) and the inter-membrane (periplasmic) space, respectively. The energy conservation in C*c*O requires a tight coupling between the transfer of electrons and substrate protons to the catalytic site, and the uptake and release of protons that are pumped across the membrane. In this paper we first describe the structure and catalytic cycle of C*c*O and then discuss in more detail results that provide insights into the mechanism by which the enzyme controls the timing and direction of the internal electron and proton-transfer reactions.

Among the most widely studied C*c*Os are cytochromes aa_3 from bovine heart mitochondria, and from the bacteria *Rhodobacter (R.) sphaeroides* and *Paracoccus (P.) denitrificans*. While the mitochondrial enzyme consists of 13 subunits [3,4], these

Abbreviations: C*c*O, cytochrome *c* oxidase; Cu_A, Cu_B, copper A and B, respectively; **R**, C*c*O with a fully reduced catalytic site (i.e. heme a_3 and Cu_B are both reduced); **A**, C*c*O with a reduced catalytic site and with O_2 bound to the reduced heme a_3; $\mathbf{P_M}$, $\mathbf{P_R}$, the "peroxy" intermediate formed at the catalytic site upon reaction of C*c*O with O_2, with only the catalytic site reduced (i.e. with two electrons) and where also heme *a* is reduced (i.e. in the four-electron reduced C*c*O), respectively; **F**, "oxo-ferryl" intermediate; **O, $\mathbf{O_H}$**, fully-oxidized enzyme in the relaxed and "activated" states, respectively; *N*-side, negative side of the membrane; *P*-side, positive side of the membrane. If not indicated otherwise the amino-acid residue numbering refers to the *R. sphaeroides* C*c*O (cytochrome aa_3) structure

* Corresponding authors.
E-mail addresses: r-gennis@uiuc.edu (R.B. Gennis), peterb@dbb.su.se (P. Brzezinski).

0005-2728/$ - see front matter © 2006 Elsevier B.V. All rights reserved.
doi:10.1016/j.bbabio.2006.05.020

bacterial enzymes are composed of four subunits [5,6]. The sequence similarity of the catalytic core consisting of subunits I–III between the bacterial enzymes and the corresponding subunits in the bovine heart enzyme is very high [7–10], and about 50% of the amino-acid residues are identical (for a description of heme-copper oxidases from different organisms as well as evolutionary aspects, see [11–14]).

Even though the minimal functional unit (i.e. oxygen reducing and proton pumping) consists of only subunits I and II ([15,6–18], see also [19]), during the enzyme turnover, the two-subunit enzyme is irreversibly inactivated ("suicide inactivation"), which indicates that subunit III is required for maintaining the structural integrity of the redox-active sites ([20], see also [17]). In addition, subunit III has also been suggested to participate in channeling oxygen to the binuclear site [21,22].

2. Structure

The crystal structures of C*c*O (cytochrome aa_3) from bovine heart [3,4,23] and from the bacterium *P. denitrificans* [5,24] were first presented in 1995. In the following years three-dimensional structures of cytochrome ba_3 from *Thermus (T.) thermophilus* [25], cytochrome bo_3 from *E. coli* [26], and C*c*O from *R. sphaeroides* [6] were presented.

The four-subunit *R. sphaeroides* C*c*O, which is primarily discussed in this paper, has a total molecular weight of ~130 kDa. Three of the redox-active cofactors, hemes *a* and a_3 (hence the name cytochrome aa_3) and copper B (Cu_B) are found in subunit I while the fourth cofactor, copper A (Cu_A), is found in subunit II. Subunit I consists of 12 membrane-spanning segments that are largely helical in their secondary structure (Fig. 1a). The iron of heme *a* has two axial histidine ligands while the heme a_3 iron has only one axial histidine ligand and the sixth position is used to bind external ligands such as O_2. The Cu_B ion, with three histidine ligands, is 4.6 Å away from the heme a_3 iron in the oxidized enzyme. Subunit II has two transmembrane helices, anchoring the subunit in the membrane, and it holds the dinuclear Cu_A center in its hydrophilic globular domain. The two copper ions form a mixed-valence {Cu(1.5)–Cu(1.5)} complex [27,28] and act together as a one-electron donor or acceptor. Subunit III is composed of seven transmembrane helices, arranged in two bundles separated by a large V-shaped cleft. Subunit IV consists only of one transmembrane helix, and its function is unknown.

2.1. Proton-transfer pathways

Because C*c*O is a transmembrane protein, its function as a proton pump requires proton pathways spanning the entire thickness of the membrane. In addition, the location of the oxygen-binding catalytic site in the membrane-spanning part of the protein, about 35 Å from the proton-input (*N*) side of the membrane, requires pathways for transfer of substrate protons to the catalytic site. As for many other oxidases, in the *R. sphaeroides* C*c*O structure, two proton-transfer pathways, the D- and K-pathways, connect the *N*-side solution with the catalytic site [5,6,29] (Fig. 1b). The output part of the pathway for pumped

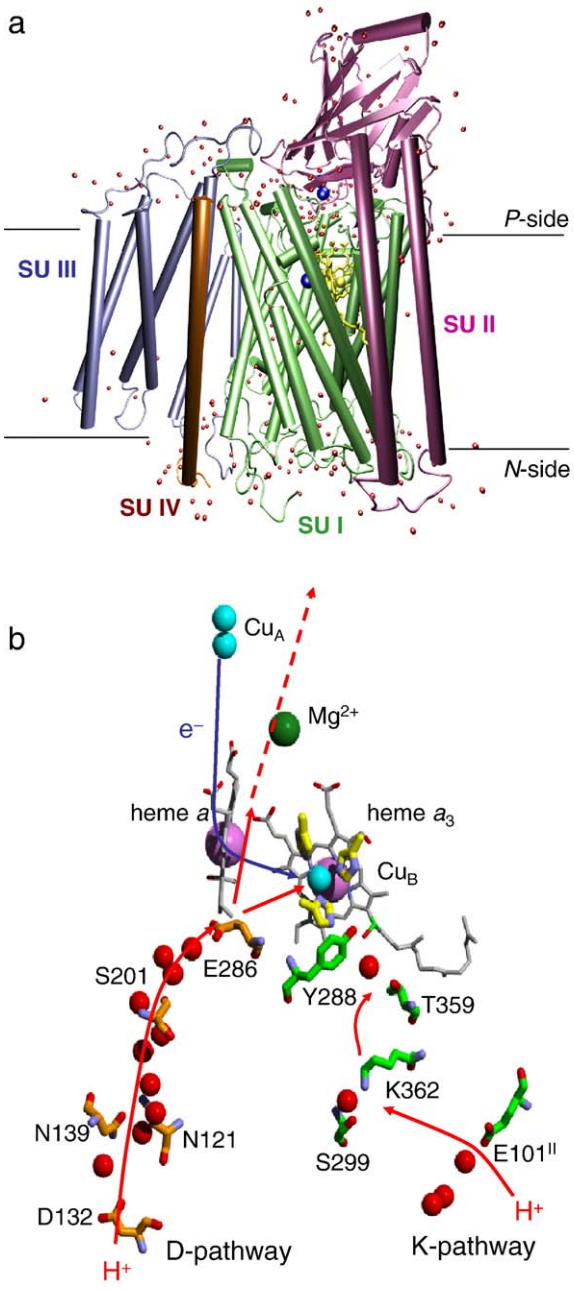

Fig. 1. (a) The overall structure of C*c*O (cytochrome aa_3) from *R. sphaeroides*. The four subunits are shown in different colors as indicated in the figure. (b) The redox-active cofactors of C*c*O and the D and K proton-transfer pathways used for uptake of substrate and pumped protons (red lines). The protons to be pumped are presumably transferred to or through the heme propionates. The proton output pathway is not known and it is only shown schematically as a dashed line. The red spheres are water molecules resolved in the X-ray crystal structure. Electrons are donated from cytochrome *c*, first to Cu_A and then sequentially to heme *a* and to the catalytic site consisting of heme a_3 and Cu_B (blue line).

protons (above the level of hemes *a* and a_3) is not apparent from an analysis of the X-ray structures. However, results from experimental and theoretical calculations indicate that the pathway extends *via* the region including residues Arg 481 and 482, interacting with the heme propionates [5,30–38]. Analyses of the C*c*O crystal structures suggest that the region above the

heme propionates at the interface between subunits I and II contains many water molecules, so that proton transfer beyond the propionates may take a large number of alternative routes. There is also a magnesium ion (or manganese) bound in this region, which may have a structural role and also participate in the proton release [39–44].

2.1.1. The D-pathway

The D-pathway starts at the *N*-side surface at a functionally important and highly conserved aspartate residue, Asp132 [45–47]. It continues, through a hydrogen-bonded chain consisting of about ten ordered water molecules and polar residues, to another highly conserved and essential residue Glu286, which is located ~24 Å from Asp132 (Fig. 1b). This arrangement of protonatable amino-acid residues and water molecules provides a Grotthuss-type proton-transfer pathway through the membrane-spanning part of the protein. The D-pathway is used for the transfer of both substrate and pumped protons (see below), and the proton-transfer reaction has been investigated in detail using theoretical tools [37,48,49]. A possible branching point from where protons are transferred either to the catalytic site (substrate protons) or towards the heme propionates (pumped protons) is located at Glu286 [5,31,49–51]. Even though the X-ray crystal structures do not show any water molecules that would conduct the protons beyond Glu286, results from theoretical calculations indicate that two chains of disordered water molecules, not resolved in the structure, connect Glu286 with the catalytic site and an acceptor of pumped protons, respectively [36,52–55]. The bi-directional proton transfer to either one of the two sites could be assisted by conformational changes of the Glu286 side chain during catalytic turnover [5,6,50,54], or through changes in the water structure [36,55].

2.1.2. The K-pathway

The K-pathway starts presumably at residue Glu 101 in subunit II [33,56–58], and continues through a highly-conserved lysine residue, Lys362 [59,60], in the middle of the pathway (Fig. 1b), *via* Thr 359 and the hydroxyl group of heme a_3 to a tyrosine residue Tyr288, close to the oxygen-binding catalytic site. In the *R. sphaeroides* structural model there is one water molecule between Thr359 and the heme a_3 hydroxyl. The K-pathway is not hydrogen-bonded all the way through without assuming bridging water molecules that are unresolved in the X-ray crystal structure [61]. Alternatively, the lysine side-chain might move in order to provide proton connectivity between the lower and upper parts of the K-pathway [50,62].

2.1.3. H-pathway

A third pathway for pumped protons was suggested on the basis of structural analysis and mutagenesis experiments in the mitochondrial C*c*O [3,23,63,64]. The pathway is called the H-pathway after a partially conserved histidine, His456, in the *R. sphaeroides* C*c*O [65] (or E-pathway for the *P. denitrificans* enzyme, [24]). The H-pathway overlaps partly with the D-pathway described above, but instead of leading to Glu286, it continues through polar residues further away from the catalytic site, to the output side. The H-pathway is probably not functionally important in the prokaryotic oxidases [29,65–67] and one may speculate [64] that there could be different mechanisms and pathways for proton pumping in the mitochondrial and bacterial oxidases.

3. Catalytic cycle

During catalytic turnover, electrons are donated first to Cu_A and are then transferred consecutively to heme *a* and to the catalytic site consisting of heme a_3 and Cu_B. The turnover activity of the *R. sphaeroides* C*c*O is ~1600 electrons/s at pH 6.5 [10]. Spectroscopic and chemical studies have provided a reasonably clear picture of the mechanism by which O_2 is reduced to 2 H_2O during the catalytic cycle. We will describe the catalytic cycle (Fig. 2) referring to the different redox states of the catalytic site. The remaining two redox centers, heme *a* and Cu_A, are not engaged directly in the oxygen chemistry and provide the pathway for electrons to reach the catalytic site. The reaction with O_2 requires that the catalytic site be reduced by two electrons, i.e., with the catalytic site in the heme $a_3(Fe^{2+})/Cu_B^+$ state, which we refer to as the **R** (reduced) state. After O_2 binds to ferrous heme a_3 forming the "A" state (Fig. 2), the O − O bond is broken in a concerted reaction. To break the O − O bond, four electrons and at least one proton is required. Two of the electrons are donated by the heme a_3 iron (forming the ferryl state, Fe^{4+}) and one from Cu_B (which is oxidized to form Cu_B^{2+}). The source of the additional electron depends on whether heme *a* is oxidized (*i*), the long route around the circle in Fig. 2, or reduced (*ii*), the path through $\mathbf{P_R}$, when O_2 binds to the reduced catalytic site.

(i) If heme *a* is oxidized when O_2 reacts with the R state of the catalytic site, then the reaction proceeds by oxidizing a nearby amino acid, tentatively identified as Tyr288, which also provides a proton [29,68,69]. This is shown in Fig. 2 as the branch going from state **A** to $\mathbf{P_M}$.

$$\underset{\mathbf{R}\text{ state}}{\text{YOH heme } a_3Fe^{2+}\{O{-}O\}Cu_B^+} \rightarrow \underset{\mathbf{P_M}\text{ state}}{YO^{\bullet}\text{ heme } a_3\ Fe^{4+}{=}O^{2-}HO^{-}Cu_B^{2+}} \quad (2)$$

This reaction (Equation (1)) has a time constant of ~300 μs. Note that one oxygen atom is bound to the heme iron and one oxygen atom is associated with Cu_B. This reaction is a rapid 4-electron reduction of O_2, bypassing any formation of toxic reactive oxygen species (superoxide, peroxide, hydroxide radical) (see [68]). Even though the $Fe^{4+}{=}O^{2-}$ state and Tyr radical that are formed at the catalytic site are reactive, they are bound to the C*c*O and are not released. Note that the formation of $\mathbf{P_M}$ just rearranges electrons and protons that are already present at the catalytic site and does not require any additional proton or electron input.

The concerted four-electron reduction of O_2 creates a high chemical potential, which is utilized to pump protons across the membrane during each of the following four electron transfer steps, accompanied by the uptake of four substrate protons, which takes the catalytic site back to the **R** state (blue arrows Fig. 2).

The $\mathbf{P_M}$ state has a very high midpoint potential and it is readily reduced. Transfer of an electron into the catalytic site in state $\mathbf{P_M}$,

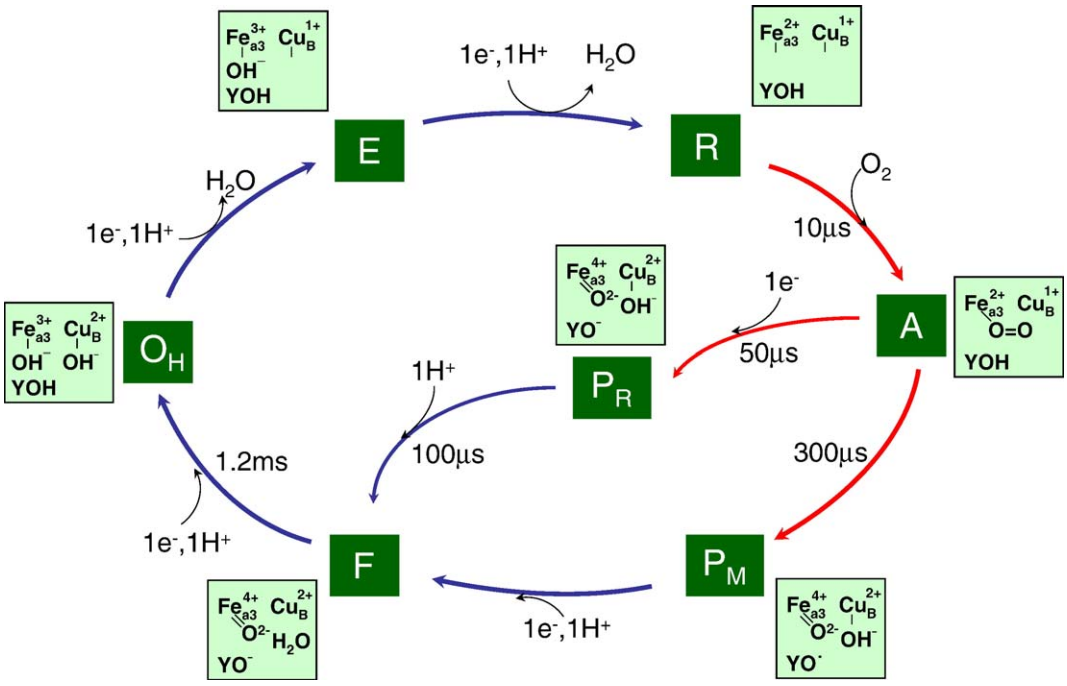

Fig. 2. The catalytic reaction of C*c*O (time constants are those observed with the *R. sphaeroides* C*c*O). The outer circle represents the reaction sequence during turnover when electrons are added one-by-one from cytochrome *c*. The reaction sequence *via* the $\mathbf{P_R}$ state is that observed during reaction of the fully reduced C*c*O (i.e. in addition to the catalytic site also heme *a* and Cu_A are reduced) with O_2. Reaction steps indicated by blue arrows are linked to proton pumping.

provided from cytochrome $c \rightarrow Cu_A \rightarrow$ heme *a*, probably results in reduction of the Tyr288 radical. Electron transfer to the catalytic site is coupled to a series of proton transfers which is thought to be the same every time an electron is transferred to the catalytic site in the reaction cycle [70,71]: two protons are taken up from the *N*-side of the protein and one is released from the *P*-side. One of the protons taken up goes to the catalytic site (substrate proton) and the other proton is pumped.

The state of the catalytic site formed by the reduction of $\mathbf{P_M}$ is denoted **F**. Transfer of an additional electron to the catalytic site is again coupled to the uptake of two protons and the release of one pumped proton. This process results in the formation of the oxidized catalytic site, denoted $\mathbf{O_H}$ where the subscript denotes an activated "high-potential" state in which it is postulated that Cu_B has a very high electrochemical potential [71–73]. The next two electron transfer reactions convert the $\mathbf{O_H}$ state to the **E** state (Cu_B reduced) and, further to the **R** state (heme a_3 and Cu_B both reduced). Each of these steps is also thought to be coupled to the uptake of two protons and release of one proton [70,71]. However, little is known about the nature of the activated $\mathbf{O_H}$ state, or the $\mathbf{O_H} \rightarrow \mathbf{E}$ and $\mathbf{E} \rightarrow \mathbf{R}$ steps of the reaction. For the purposes of this discussion it is assumed that each of the electron transfer steps to the catalytic site, $\mathbf{O_H} \rightarrow \mathbf{E}$, $\mathbf{E} \rightarrow \mathbf{R}$, $\mathbf{P_M} \rightarrow \mathbf{F}$ and $\mathbf{F} \rightarrow \mathbf{O_H}$, is associated with proton pumping by the same mechanism, but much more needs to be done experimentally to test this assumption.

(ii) If heme *a* is reduced when O_2 reacts with the **R** state of the catalytic site, then the electron required to break the O − O bond is taken from heme *a* and not from Tyr288 (Fig. 2, pathway *via* $\mathbf{P_R}$). This is the situation when the fully reduced (all four redox centers are reduced) enzyme is reacted with O_2 in the "flow-flash" reaction commonly used to study the oxidase catalysis (for review, see [74,75]). The intermediate that is observed is called the $\mathbf{P_R}$ state of the enzyme, which is spectroscopically (UV-vis) identical to $\mathbf{P_M}$ ([76], but see [77]), but presumably has a tyrosinate instead of a tyrosine radical at the catalytic site. The electron transfer from heme *a* to the catalytic site takes about 30–50 µs. After this electron transfer one proton is transferred to the catalytic site, which is observed spectroscopically as the $\mathbf{P_R} \rightarrow \mathbf{F}$ transition. In addition, the $\mathbf{P_R} \rightarrow \mathbf{F}$ transition is linked to proton pumping, i.e. in this process two protons taken up from the *N*-side and one proton released on the *P*-side [78–80], but these proton transfer reactions take place with a time constant of 100–200 µs, i.e. after the electron transfer from heme *a* to the catalytic site (Fig. 2). The clear separation for the $\mathbf{A} \rightarrow \mathbf{P_R}$ and $\mathbf{P_R} \rightarrow \mathbf{F}$ steps provides an experimental opportunity to examine the electron transfer ($\mathbf{A} \rightarrow \mathbf{P_R}$) and proton transfer ($\mathbf{P_R} \rightarrow \mathbf{F}$) events separately (see below).

In the next transition, $\mathbf{F} \rightarrow \mathbf{O_H}$, which is observed as part of the reaction of the fully reduced enzyme with O_2, the electron which was originally residing on Cu_A is transferred to the catalytic site (4th electron), forming the $\mathbf{O_H}$ state of the enzyme, as described above. The $\mathbf{F} \rightarrow \mathbf{O_H}$ transition takes about 1 ms (see e.g. [81]), and the electron and proton transfers are not clearly separable (Fig. 2). Note that in the reaction of the fully reduced enzyme with O_2 there are only two steps that are linked to proton pumping, $\mathbf{P_R} \rightarrow \mathbf{F}$ and $\mathbf{F} \rightarrow \mathbf{O_H}$ [78,80]. If additional reductant is provided to allow the $\mathbf{O_H} \rightarrow \mathbf{E}$ and $\mathbf{E} \rightarrow \mathbf{R}$ steps, then two additional protons are pumped and the enzyme is returned to the **R** state [70,71,73].

3.1. Proton-transfer reactions

As stated above, each of the electron-transfer reactions during the catalytic cycle is thought to be coupled to a similar set of

proton-transfer reactions. During the ($\mathbf{P_M}$) $\mathbf{P_R \rightarrow F}$ and the $\mathbf{F \rightarrow O_H}$ transitions, all the protons are taken up through the D-pathway [82–84]. For both the $\mathbf{O_H \rightarrow E}$ and presumably also for the $\mathbf{E \rightarrow R}$ transitions, it appears that the substrate protons are delivered to the catalytic site through the K-pathway [82,84–87]. Since much more is known about the $\mathbf{P_R \rightarrow F}$ and the $\mathbf{F \rightarrow O_H}$ transitions, the proton transfers associated with these transitions will be discussed. These proton transfer steps are shown schematically in Fig. 3. Although the elementary steps of proton transfers are the same for these two transitions, the chemistry is distinct and, in consequence, there are differences in rates of reaction, the rate-limiting steps and even, possibly, the order of events. Moreover, the solvent deuterium kinetic isotope effects (KIE) [51,88,89] and activation energies are different for the $\mathbf{P_R \rightarrow F}$ and $\mathbf{F \rightarrow O}$ transitions. A comparison of the specific reaction steps of these transitions provides important mechanistic insights into the function of C*c*O and the mechanism of proton pumping. Below, the sequence of the proton-transfer reactions is outlined and discussed in detail.

3.1.1. Proton uptake

(*i*) Protonation of Asp132, at the entrance of the D-pathway, from the bulk medium on the *N*-side of the protein: The rate of proton transfer from the bulk solution to the protonatable groups on the protein surface near the entrance of the D-pathway is presumably diffusion limited and designated in Fig. 3 as k_{diff}. These groups form a proton-collecting antenna [90–92] thereby enhancing the protonation rate of Asp132 (discussed in more detail below).

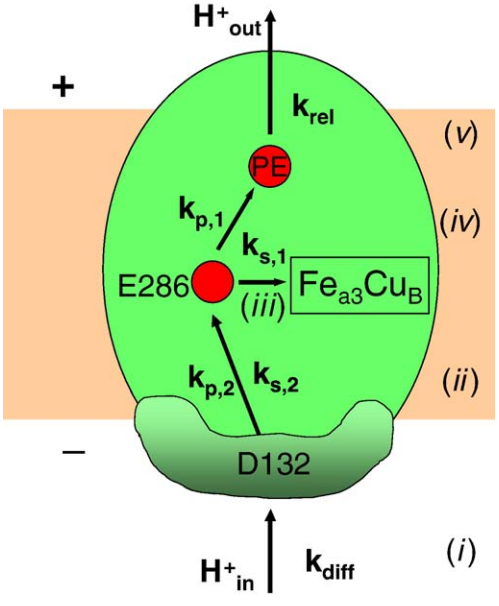

Fig. 3. Schematic illustration showing proton-transfer reactions in C*c*O: (*i*) proton uptake by Asp132 at the negative surface of the enzyme. A "proton antenna" is indicated on the surface. (*ii*) Internal proton transfers from Asp132 to Glu286, within the D pathway. (*iii*) Internal proton transfer from Glu286 to the catalytic site. (*iv*) Internal proton transfer to a proton acceptor in the "exit" pathway. (*v*) Proton release to the positive side of the membrane. The specific proton-transfer reactions and their rate constants are discussed in the text.

3.1.2. Intramolecular proton transfers

(*ii*) Proton transfer from Asp132 to Glu286 at the "top" of the D-pathway: This step must occur twice during each transition, once for the substrate proton and once for the "pumped proton". The rate constants for the pumped and substrate proton transfers to refill Glu286 are designated $k_{p,2}$ and $k_{s,2}$ (Fig. 3).

(*iii*) Proton transfer from Glu286 to the catalytic site (substrate protons), indicated as $k_{s,1}$.

(*iv*) Proton transfer from Glu286 to a proton acceptor (PE, "pumping element") in the "exit channel" (pumped proton), designated as $k_{p,1}$: One candidate for the initial proton-accepting group is the D-ring propionate of heme a_3.

3.1.3. Proton release

(*v*) Proton release from the exit channel to the bulk medium on the *P*-side of the protein, designated k_{rel}.

3.2. The $P_R \rightarrow F$ transition

A schematic of the free energy changes during the transition $\mathbf{A \rightarrow P_R \rightarrow F}$ is shown in Fig. 4a. The $\mathbf{P_R \rightarrow F}$ transition ($\tau \cong 100$ μs), which is linked to proton pumping, involves proton transfer without simultaneous electron transfer. The electron transfer ($\tau = 30$–50 μs) resulting in the formation of $\mathbf{P_R}$ precedes the proton transfer. Hence, an investigation of the $\mathbf{P_R \rightarrow F}$ transition provides detailed information about the sequence of proton-transfer reactions during a pumping cycle. The results from kinetic studies indicate that proton transfer from solution to the catalytic site involves transient deprotonation of Glu286 (see Fig. 1b). The residue is in rapid proton equilibrium with the bulk solution and the observed $\mathbf{P_R \rightarrow F}$ rate (k_{PF}) is determined by the fraction of protonated Glu286 (α(EH)) multiplied by the proton-transfer rate from Glu286 to the catalytic site, k_H, which has a value of about 10^4 s^{-1} ($\tau = 100$ μs). This proton transfer determines the maximum rate of the $\mathbf{P_R \rightarrow F}$ transition, which can be described by a simple Henderson–Hasselbalch equation with a single titratable group with a pK_a of 9.4:

$$k_{PF} = \alpha(\mathrm{EH})k_H = \frac{k_H}{1 + 10^{\mathrm{pH}-\mathrm{p}K_{E286}}} \quad (3)$$

If proton uptake through the D-pathway is blocked near the protein surface, for example by replacement of Asp132 (see Fig. 1b) by a non-protonatable residue, the **F** intermediate is still formed, but the proton needed for the $\mathbf{P_R \rightarrow F}$ transition to take place is transferred internally from Glu286 (also with a time constant of ~100 μs), leaving the residue transiently deprotonated.

Because the $\mathbf{P_R \rightarrow F}$ transition is associated with proton pumping, it involves the uptake of two protons from the *N*-side and release of one proton to the *P*-side of the membrane, and is not simply the proton transfer from Glu286 to the catalytic site. A comparison of the proton uptake and release rates in C*c*O reconstituted in lipid vesicles in H_2O and D_2O, respectively, showed that in the reaction of the fully reduced enzyme with O_2, proton uptake displays a KIE of ~2 while the proton release displays a KIE of ~7 [93]. Hence, in D_2O, the uptake of two

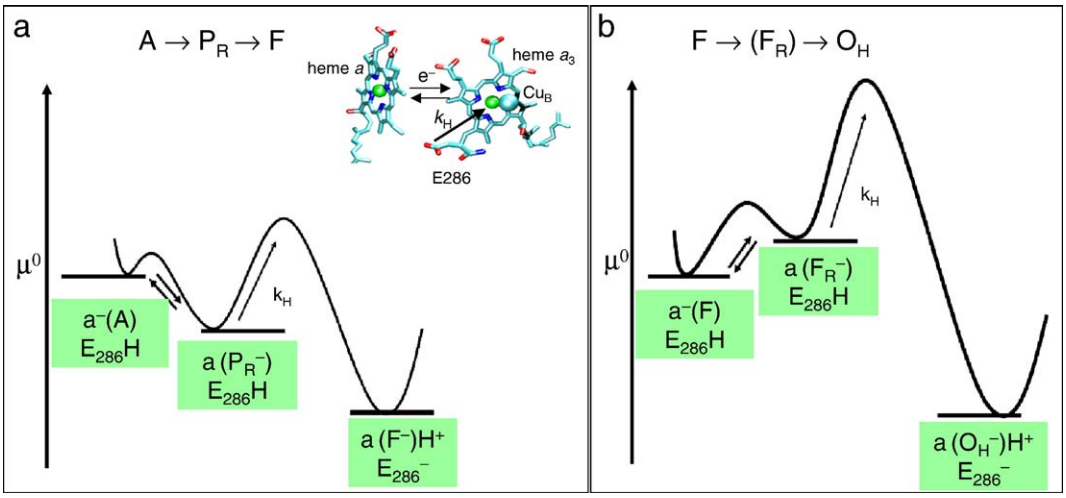

Fig. 4. Schematic free energy profiles of the $\mathbf{A \rightarrow P_R \rightarrow F}$ and the $\mathbf{F \rightarrow O_H}$ transitions that are measured in the flow-flash reaction monitoring the single turnover of the oxidase. Both transitions represent the transfer of an electron and a proton to the catalytic site. The state of the catalytic site is denoted by (**A**), ($\mathbf{P_R}$), (**F**), etc. and the electron and proton transferred is notated explicitly. The proton comes initially from Glu286, which is transiently deprotonated but rapidly reprotonated (not shown).

protons occurs first, and only afterwards is the release of one proton observed (see Fig. 5) [93]. Using the schematic illustration in Fig. 3, in D_2O $k_{s,1}$, $k_{s,2}$, $k_{p,1}$ and $k_{p,2}$ are larger than k_{rel}. There must be two protonatable sites available prior to proton release. One proton vacancy is certainly created by the chemistry at the catalytic site ($k_{s,1}$ followed by $k_{s,2}$), and the second presumably reflects a proton acceptor, connected to the exit channel ($k_{p,1}$ followed by $k_{p,2}$), whose pK_a has been transiently increased.

Recently, time-resolved electrical measurements have shown that there is some charge movement across the membrane associated with the $\mathbf{A \rightarrow P_R}$ transition, i.e. before any proton uptake or release from/to solution [94]. The interpretation is that this represents proton transfer from Glu286 to the exit channel proton acceptor ($k_{p,1}$ in Fig. 3), coincident in time with the electron transfer from heme *a* to the catalytic site. Presumably, this is then followed by the uptake of two protons, and then by the proton release step.

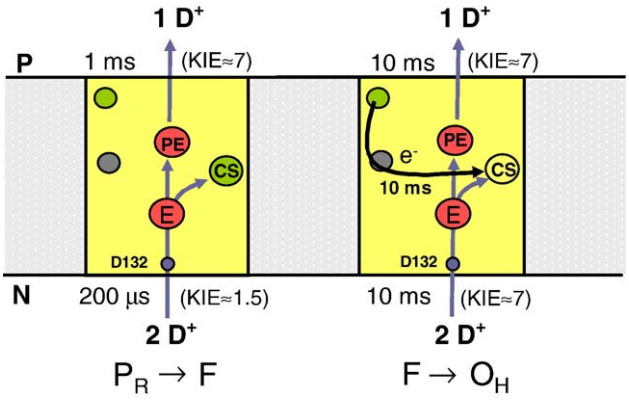

Fig. 5. Schematic of the proton-transfer reactions during $\mathbf{P_R \rightarrow F}$ and $\mathbf{F \rightarrow O_H}$ in D_2O and the solvent kinetic deuterium isotope effects (KIE). The time constants are those observed in D_2O (c.f. time constant in H_2O in Fig. 2). PE is a "pumping element", which controls the uptake and release of the pumped protons. E is Glu286 and CS is the catalytic site. Redox sites in green are reduced (in the $\mathbf{P_R}$ state the catalytic site has excess electrons).

3.3. The $F \rightarrow O_H$ transition

Whereas the $\mathbf{P_R \rightarrow F}$ transition occurs at $\tau \cong 100$ μs, the $\mathbf{F \rightarrow O_H}$ transition is much slower, $\tau \cong 1$ ms. This is presumably because, in addition to the same series of proton-transfer reactions as discussed above for the $\mathbf{P_R \rightarrow F}$ transition, the $\mathbf{F \rightarrow O_H}$ transition also includes the electron transfer to the catalytic site [95]. Thus, in contrast to the $\mathbf{A \rightarrow P_R \rightarrow F}$ sequence, in which electron transfer clearly precedes proton transfer, electron transfer to the **F** state does not proceed to any measurable extent prior to the coupled proton transfer. Consequently, there is no accumulation of an intermediate form of **F**, which is reduced (equivalent to $\mathbf{P_R}$) prior to the proton transfer to the catalytic site. We can postulate that this species ($\mathbf{F_R}$) likely forms but is not stable relative to **F** and, therefore, never observable. In analogy with Equation 3 above, the rate of the $\mathbf{F \rightarrow O_H}$ transition is determined by the fraction of protonated Glu286 (α(EH)) multiplied by the proton-transfer rate from Glu286 to the catalytic site, k_H, (10^4 s^{-1}) and the fraction $\mathbf{F_R}$, γ(F_R) [95]:

$$k_{FO} = \alpha(EH)\gamma(F_R)\cdot k_H = \gamma(F_R)\frac{k_H}{1+10^{pH-pK_{E286}}} \quad (4)$$

This situation is schematically shown in Fig. 4b. The observed rate of proton transfer to the catalytic site (formally $\mathbf{F_R \rightarrow O_H}$) is dependent on the amount of $\mathbf{F_R}$ that is formed and, since this is never present in large amount, the observed rate of formation of $\mathbf{O_H}$ is slow (~1 ms). Evidently, the $\mathbf{A/P_R}$ redox couple has a higher electrochemical midpoint potential than $\mathbf{F/F_R}$ as indicated in Fig. 4. This is plausible since the chemistry occurring at the catalytic site during these two reactions is quite different. In the case of $\mathbf{A \rightarrow P_R}$, the electron reduces O_2 as the O − O bond is split. During the postulated electron transfer reaction $\mathbf{F \rightarrow F_R}$, the ferryl heme a_3 ($Fe^{4+}{=}O^{2-}$) is reduced to ferric heme a_3 (Fe^{3+} O^{2-}), which is not expected to be a stable species without the proton to convert the O^{2-} to HO^- (see Fig. 4b). Not surprisingly, the

activation energy of the $\mathbf{P_R \rightarrow F}$ and $\mathbf{F \rightarrow O_H}$ transitions are different (see Fig. 6) (see also [96]).

The amount of the putative $\mathbf{F_R}$ that is formed can be decreased by increasing the midpoint potential of Cu_A, which is accomplished by the Met263Leu mutation in subunit II of the oxidase [97]. Since the rate of the $\mathbf{F \rightarrow O_H}$ transition depends on the concentration of $\mathbf{F_R}$, the effect of this mutation is to slow the $\mathbf{F \rightarrow O_H}$ rate by 100-fold [98].

During the $\mathbf{F \rightarrow O_H}$ transition both the electron and substrate proton transfer to the catalytic site, as well as the uptake of pumped protons, all display the same, large KIE of ~7 (measured in the reaction of the fully reduced enzyme with O_2) [88,89,93,99]. Comparison with the data from the $\mathbf{P_R \rightarrow F}$ transition in which the proton release step is identified as having a KIE ~ 7, suggests that the rate-limiting step of the $\mathbf{F \rightarrow O_H}$ transition is the release of the pumped proton (see Fig 5). In the Met263Leu (subunit II) mutant C*c*O, in which the rate of the $\mathbf{F \rightarrow O_H}$ transition is slowed by 100-fold, the KIE of the transition is 7, as in the wild type C*c*O, and proton-pumping stoichiometry is normal despite the slow rate. Presumably, the rate is still limited by the proton release [51,93].

If, on the other side, proton uptake from solution into the D pathway is slowed by introduction of a mutation, proton pumping becomes uncoupled from O_2 reduction [46]. This situation is observed, for example, in the Asp132Asn mutant C*c*O where proton uptake into the D-pathway is slowed by a factor of ~1000 to ~1 s^{-1} [100]. Presumably, in this case the initial deprotonation of Glu286 to form state **F** leaves the residue in an unprotonated state such that transfer of the pumped proton is not possible. Interestingly, in the Asp132Asn mutant C*c*O the KIE of the $\mathbf{F \rightarrow O_H}$ transition rate is ~1 (unpublished results), which further supports the conclusion that the large KIE of ~7 in the wild-type C*c*O is associated with transfer of the pumped proton.

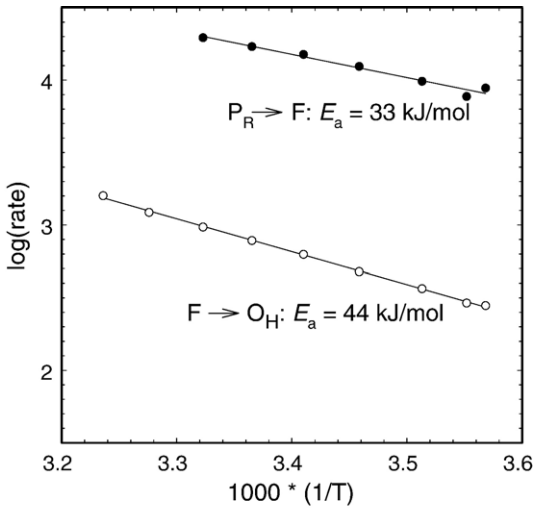

Fig. 6. Temperature dependence of the $\mathbf{P_R \rightarrow F}$ and $\mathbf{F \rightarrow O_H}$ transition rates measured with the *R. sphaeroides* C*c*O. Conditions: ~1 μM C*c*O, 0.1 HEPES–KOH pH 7.6, 0.1% dodecyl β-D maltoside, 1 mM O_2. (for a description of the experimental system, see [62]).

It is also possible to block proton uptake into the D-pathway of the bovine oxidase by treating the purified enzyme in such a way as to convert the dimeric enzyme to monomers. The reason why proton uptake is influenced by this treatment is not known, but the phenomenon is clear at high pH. The $\mathbf{F \rightarrow O_H}$ transition was studied by photoreduction using the monomeric bovine oxidase at alkaline pH [101,102]. Remarkably, a proton release is clearly observed coincident with the electron transfer to the catalytic site, and the proton uptake is substantially delayed. One must conclude that, at the very least, there are two internal protons available within the monomeric bovine C*c*O in order to explain proton release and proton delivery to the active site occurring prior to proton uptake. Possibly, in the monomeric enzyme, the equivalent to Asp132 at the entrance of the D-pathway (see Fig. 3) is stabilized in a protonated state and the rate of proton transfer from bulk solution to the D-pathway is slow. In this case, Asp132 could readily provide a proton to Glu286, but proton uptake from solution *via* Asp132 is delayed. In this case, and in contrast to the observation of the $\mathbf{P_R \rightarrow F}$ transition, proton release can occur prior to proton uptake from solution.

The order and timing of proton-transfer reactions in C*c*O have also been investigated through time-resolved electrical measurements, which are used to examine the movement of charges across the membrane during the catalytic cycle and, specifically, for the $\mathbf{F \rightarrow O_H}$ transition. This is studied by preparing the **F** state by reacting C*c*O with hydrogen peroxide, and then injecting one electron into the enzyme using a Ru complex [103]. The data show that proton movements across the membrane bilayer occur in two phases with time constants of ~0.5 ms and ~1.5 ms. By comparing the data for the wild type *R. sphaeroides* C*c*O and a mutant which does not pump protons, it was shown that the first of the phases is due to proton movements associated with the pumping mechanism, and this phase is not observed when there is no proton pumping [104]. Presumably, the first event corresponds to proton transfer from Glu286 to the exit channel. The second (1.5 ms) phase may correspond to the transfer of the proton to the catalytic site, reprotonation of Glu286 and finally release of the proton from the exit channel.

3.4. Proton uptake at the surface

At pH 7 C*c*O is able to transfer up to ~1500 electrons s^{-1}. At this maximum rate, on the average more than 2200 protons s^{-1} (at least 6 out of the 8 protons per turnover, see above) are transferred through the D-pathway, which corresponds approximately to the diffusion limit for protons in water ($4 \cdot 10^{10}$ M^{-1} $s^{-1} \times 10^{-7}$ M protons = 4000 s^{-1}, at pH 7). Much faster rates are observed for the specific reaction steps where, for example, during the $\mathbf{P_R \rightarrow F}$ transition the proton-uptake rate constant is ~10^4 s^{-1} up to pH 8.5 [105], which gives an apparent second-order rate constant of ~$3 \cdot 10^{12}$ M^{-1} s^{-1}. Furthermore, an analysis of these data indicated that proton transfer within the D-pathway from Asp132 to Glu286, $k_{s,2}$ (and presumably also $k_{p,2}$, see Fig. 3) is even faster than 10^4 s^{-1} [105] and not rate limiting for proton uptake to the catalytic site. Rapid proton delivery to the entrance of the D-

pathway has been speculated to be facilitated by a proton-collecting antenna composed of protonatable groups surrounding the orifice of a proton pathway [90], schematically illustrated in Fig. 3. Some of the components of this antenna are most likely located at SU III, which extends to the area around Asp132 at SU I [106].

4. Energetics of the proton pump

Cytochrome *c* oxidase is capable of operating against a membrane potential of about +220 mV in active mitochondria. The work potential from the overall reaction (4 cyt c^{2+} + $4H^+ + O_2 \rightarrow 4$ cyt $c^{3+} + 2H_2O$), which is once around the catalytic cycle (Fig. 2), is about −2200 mV. Hence, the work performed by C*c*O when moving charges against the membrane electric potential accounts for 8×+220 mV=+1760 mV, i.e. ~80% efficiency. The step during which O_2 binds to the reduced catalytic site (producing the **A** state; see Fig. 2) and reacts to form the initial product, $\mathbf{P_M}$, is not coupled to proton pumping or any charge translocation across the membrane [78,80]. Presumably, this reaction proceeds without dissipating much of the work potential that is needed in the subsequent four electron transfer steps [69], $\mathbf{O_H \rightarrow E}$, $\mathbf{E \rightarrow R}$, $\mathbf{P_M/P_R \rightarrow F}$ and $\mathbf{F \rightarrow O_H}$. One might expect that the free energy available to do work is distributed approximately evenly among the four electron-transfer steps of the catalytic cycle [72]. The free-energy changes for these individual steps are not known, but in Fig. 7 (left side) a schematic free energy diagram is shown for the steps in the reaction cycle (Fig. 2) (iso-energetic assumption).

Anaerobic electrochemical titrations can, in principle, be used to measure the work potential of the two steps prior to the reaction with O_2, namely $\mathbf{O \rightarrow E}$ and $\mathbf{E \rightarrow R}$, where we refer now to the form of the oxidized enzyme prepared in the laboratory under equilibrium conditions (i.e., not during turnover) as "**O**" without the subscript "H". The electron transfer from cytochrome *c* to the catalytic site (either $\mathbf{O \rightarrow E}$ or $\mathbf{E \rightarrow R}$) yields no more than about − 100 mV change in free energy [72], far less than required to drive two charges across the membrane against the operating membrane potential (2×220 mV=+440 mV) (See Fig. 7, right side). Indeed, the **R** state, with the two-electron reduced heme a_3/Cu_B center is not more stable than having the state with the two electrons on heme *a* and Cu_B [107]. This is the reason why it has been postulated that the form of the oxidized enzyme that is present during steady state turnover is somehow different and may have midpoint potentials for the metals in the catalytic site that are much higher than measured under equilibrium conditions [71–73]. Presumably, the high potential form of the oxidized enzyme, $\mathbf{O_H}$, is unstable and, unless an electron is transferred to the catalytic site quickly after the formation of $\mathbf{O_H}$, the free energy is dissipated as heat ($\mathbf{O_H \rightarrow O}$). This classifies C*c*O as a hysteric enzyme, i.e. its properties are dependent upon its history, e.g., the length of time after oxidation by O_2 before the next electron is delivered to the catalytic site. Indeed, there is considerable evidence that the catalytic site of the oxidized enzyme can be prepared in different forms with very distinct behavior [108], though the chemical explanation is not clear. These various enzyme forms have been referred to as "resting" (or slow) versus "pulsed" (or fast) [109]. Presumably, the

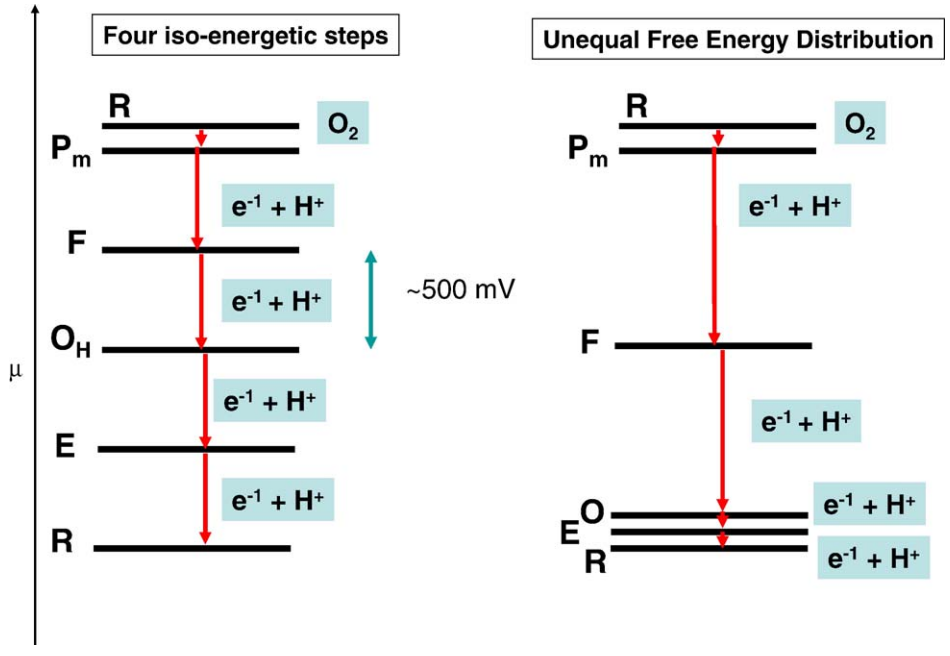

Fig. 7. Free energy diagram showing schematically the distribution of the free energy from the four-electron reduction of O_2 to 2 H_2O by C*c*O. The starting point is the two-electron reduced form of the enzyme, **R**, which reacts to form intermediate $\mathbf{P_M}$. This is then reduced by four electrons to bring the system back to the **R** state. In the scheme on the right, it is assumed that most of the free energy is expended in the $\mathbf{P_M \rightarrow F}$ and the $\mathbf{F \rightarrow O}$ steps. The $\mathbf{O \rightarrow E}$ and $\mathbf{E \rightarrow R}$ transitions are not sufficiently energy yielding to drive proton pumping. In such a scheme, each step could still be coupled to proton pumping, in principle, but the free energy from the $\mathbf{P_M \rightarrow F}$ and $\mathbf{F \rightarrow O}$ steps would be needed to "pull" the less favored $\mathbf{O \rightarrow E}$ and $\mathbf{E \rightarrow R}$ transitions. In the scheme on the left it is assumed that the free energy drop is about equal for each of the four one-electron transfers to the catalytic site. Each step is independently associated with proton pumping against a proton motive force.

putative activated form now postulated ($\mathbf{O_H}$) is either equivalent to the pulsed enzyme or related to it in some manner.

Experimental work to demonstrate the existence of $\mathbf{O_H}$ has not yielded consistent results. The Wikström laboratory has demonstrated that two protons are pumped across a vesicle membrane coincident with the two-electron reduction of the enzyme, but only if the reduction immediately follows the oxidation of the enzyme, $\mathbf{O_H \rightarrow E \rightarrow R}$ [71,73]. The same group has also used electrometric methods to show that electron injection into the recently oxidized enzyme ($\mathbf{O_H}$) generates a voltage across the membrane that is similar to what has previously been observed with $\mathbf{F \rightarrow O}$ [71]. The data were interpreted to demonstrate that each of the four electron transfer reactions drives the same amount of charge across the membrane, and that each step proceeds to essentially 100% formation of the product ($\mathbf{O_H \rightarrow E}$, $\mathbf{E \rightarrow R}$, $\mathbf{P_M \rightarrow F}$ and $\mathbf{F \rightarrow O_H}$). Electrometric data have also been published by Michel and coworkers showing that the $\mathbf{E \rightarrow R}$ transition is coupled to proton pumping [110]. The actual work potential for each step remains unknown in all these experiments. Obviously, the energetics of the C*c*O catalytic cycle is an area requiring further research to clarify these important aspects of how the enzyme operates under physiological conditions.

5. Summary

In this review, we have discussed the structural elements involved in proton transfer in C*c*O, as well as the order and timing of these reactions. During C*c*O turnover, electrons are delivered one-by-one to the catalytic site, and the data now suggest that each of these electron transfer events is mechanistically coupled to proton pumping. Proton pumping measurements in vitro are all performed without any electrochemical potential opposing the charge movement across the membrane, and it has not yet been demonstrated that each of the four steps has sufficient work potential to drive two charges across the membrane against a 220 mV potential. At this point it is a reasonable working hypothesis that each step involves the same sequence of events, resulting in proton pumping. The details of the chemistry occurring at the active site is not critical, and is different for each of the electron transfer reactions. The important property when considering proton pumping appears to be the driving force for electron transfer from heme *a* to the heme a_3/Cu_B catalytic site. The charge redistribution initiates a sequence of proton transfers. Conformational changes, such as might result from the deprotonation of Glu286, for example [111], may play an important role, and is a promising research direction. The role of redistribution or reorientation of water may be another important factor defining the sequence of events, as appears to be the case in bacteriorhodopsin [112]. Future progress is likely to depend on improved time-resolved assays to reveal the structural changes that occur during a proton pumping transition such as the $\mathbf{A \rightarrow P_R \rightarrow F}$ or $\mathbf{F \rightarrow O}$ transition. Although progress has been substantial in the past several years, an understanding of how this pump operates and what makes it unidirectional still evades us. What are the proton acceptors in the "exit" pathway, and what is this pathway? Which steps are electrogenic? What are the pK_a changes that occur and what determines the order of events during turnover? What is the nature of the proposed "high potential" $\mathbf{O_H}$ state of the enzyme and what differentiates this structurally from the resting "**O**" state? These are just a few of the questions to be addressed, and it is very likely that answers will be forthcoming.

References

[1] M.K.F. Wikström, Proton pump coupled to cytochrome *c* oxidase in mitochondria, Nature 266 (1977) 271–273.

[2] G. Antonini, F. Malatesta, P. Sarti, M. Brunori, Proton pumping by cytochrome oxidase as studied by time-resolved stopped-flow spectrophotometry, Proc. Natl. Acad. Sci. U. S. A. 90 (1993) 5949–5953.

[3] T. Tsukihara, H. Aoyama, E. Yamashita, T. Tomizaki, H. Yamaguchi, K. Shinzawa-Itoh, R. Nakashima, R. Yaono, S. Yoshikawa, The whole structure of the 13-subunit oxidized cytochrome *c* oxidase at 2.8 Å, Science 272 (1996) 1136–1144.

[4] T. Tsukihara, H. Aoyama, E. Yamashita, T. Tomizaki, H. Yamaguchi, K. Shinzawa-Itoh, R. Nakashima, R. Yaono, S. Yoshikawa, Structures of metal sites of oxidized bovine heart cytochrome *c* oxidase at 2.8 Å, Science 269 (1995) 1069–1074.

[5] S. Iwata, C. Ostermeier, B. Ludwig, H. Michel, Structure at 2.8 Å resolution of cytochrome *c* oxidase from *Paracoccus denitrificans*, Nature 376 (1995) 660–669.

[6] M. Svensson-Ek, J. Abramson, G. Larsson, S. Törnroth, P. Brzezinski, S. Iwata, The X-ray crystal structures of wild-type and EQ(I-286) mutant cytochrome *c* oxidases from *Rhodobacter sphaeroides*, J. Mol. Biol. 321 (2002) 329–339.

[7] J. Cao, J. Shapleigh, R. Gennis, A. Revzin, S. Ferguson-Miller, The gene encoding cytochrome *c* oxidase subunit II from *Rhodobacter sphaeroides*; comparison of the deduced amino acid sequence with sequences of corresponding peptides from other species, Gene 101 (1991) 133–137.

[8] J. Cao, J. Hosler, J. Shapleigh, A. Revzin, S. Ferguson-Miller, Cytochrome aa3 of *Rhodobacter sphaeroides* as a model for mitochondrial cytochrome *c* oxidase. The coxII/coxIII operon codes for structural and assembly proteins homologous to those in yeast, J. Biol. Chem. 267 (1992) 24273–24278.

[9] J.P. Shapleigh, R.B. Gennis, Cloning, sequencing and deletion from the chromosome of the gene encoding subunit I of the aa3-type cytochrome *c* oxidase of *Rhodobacter sphaeroides*, Mol. Microbiol. 6 (1992) 635–642.

[10] J.P. Hosler, J. Fetter, M.M. Tecklenburg, M. Espe, C. Lerma, S. Ferguson-Miller, Cytochrome aa3 of *Rhodobacter sphaeroides* as a model for mitochondrial cytochrome *c* oxidase. Purification, kinetics, proton pumping, and spectral analysis, J. Biol. Chem. 267 (1992) 24264–24272.

[11] M.M. Pereira, M. Santana, M. Teixeira, A novel scenario for the evolution of haem-copper oxygen reductases, Biochim. Biophys. Acta, Bioenerg. 1505 (2001) 185–208.

[12] J.A. García-Horsman, B. Barquera, J. Rumbley, J. Ma, R.B. Gennis, The superfamily of heme-copper respiratory oxidases, J. Bacteriol. 176 (1994) 5587–5600.

[13] J. Vanderoost, A.P.N. Deboer, J.W.L. Degier, W.G. Zumft, A.H. Stouthamer, R.J.M. Vanspanning, The heme-copper oxidase family consists of 3 distinct types of terminal oxidases and is related to nitric-oxide reductase, FEMS Microbiol. Lett. 121 (1994) 1–9.

[14] J. Hendriks, U. Gohlke, M. Saraste, From NO to OO: nitric oxide and dioxygen in bacterial respiration, J. Bioenerg. Biomembranes 30 (1998) 15–24.

[15] T. Haltia, M. Saraste, M. Wikström, Subunit III of cytochrome *c* oxidase is not involved in proton translocation: a site-directed mutagenesis study, EMBO J. 10 (1991) 2015–2021.

[16] R.W. Hendler, K. Pardhasaradhi, B. Reynafarje, B. Ludwig, Comparison of energy-transducing capabilities of the 2-subunit and 3-subunit

cytochromes Aa3 from paracoccus-denitrificans and the 13-subunit beef-heart enzyme, Biophys. J. 60 (1991) 415–423.
[17] M.R. Bratton, L. Hiser, W.E. Antholine, C. Hoganson, J.P. Hosler, Identification of the structural subunits required for formation of the metal centers in subunit I of cytochrome *c* oxidase of *Rhodobacter sphaeroides*, Biochemistry 39 (2000) 12989–12995.
[18] F. Malatesta, G. Antonini, P. Sarti, M. Brunori, Transient kinetics of subunit-III-depleted cytochrome *c* oxidase, Biochem. J. 234 (1986) 569–572.
[19] D.A. Thompson, L. Gregory, S. Ferguson-Miller, Cytochrome *c* oxidase depleted of subunit III: proton-pumping, respiratory control, and pH dependence of the midpoint potential of cytochrome a, J. Inorg. Biochem. 23 (1985) 357–364.
[20] M.R. Bratton, M.A. Pressler, J.P. Hosler, Suicide inactivation of cytochrome *c* oxidase: catalytic turnover in the absence of subunit III alters the active site, Biochemistry 38 (1999) 16236–16245.
[21] S. Riistama, A. Puustinen, A. Garcia-Horsman, S. Iwata, H. Michel, M. Wikström, Channelling of dioxygen into the respiratory enzyme, Biochim. Biophys. Acta 1275 (1996) 1–4.
[22] L. Salomonsson, A. Lee, R.B. Gennis, P. Brzezinski, A single-amino-acid lid renders a gas-tight compartment within a membrane-bound transporter, Proc. Natl. Acad. Sci. U. S. A. 101 (2004) 11617–11621.
[23] S. Yoshikawa, K. Shinzawa-Itoh, R. Nakashima, R. Yaono, E. Yamashita, N. Inoue, M. Yao, M.J. Fei, C.P. Libeu, T. Mizushima, H. Yamaguchi, T. Tomizaki, T. Tsukihara, Redox-coupled crystal structural changes in bovine heart cytochrome *c* oxidase, Science 280 (1998) 1723–1729.
[24] C. Ostermeier, A. Harrenga, U. Ermler, H. Michel, Structure at 2.7 Å resolution of the *Paracoccus denitrificans* two-subunit cytochrome *c* oxidase complexed with an antibody FV fragment, Proc. Natl. Acad. Sci. U. S. A. 94 (1997) 10547–10553.
[25] T. Soulimane, G. Buse, G.P. Bourenkov, H.D. Bartunik, R. Huber, M.E. Than, Structure and mechanism of the aberrant ba_3-cytochrome *c* oxidase from *Thermus thermophilus*, EMBO J. 19 (2000) 1766–1776.
[26] J. Abramson, S. Riistama, G. Larsson, A. Jasaitis, M. Svensson-Ek, L. Laakkonen, A. Puustinen, S. Iwata, M. Wikström, The structure of the ubiquinol oxidase from *Escherichia coli* and its ubiquinone binding site, Nat. Struct. Biol. 7 (2000) 910–917.
[27] M. Karpefors, C.E. Slutter, J.A. Fee, R. Aasa, B. Källebring, S. Larsson, T. Vänngård, Electron paramagnetic resonance studies of the soluble CuA protein from the cytochrome ba_3 of *Thermus thermophilus*, Biophys. J. 71 (1996) 2823–2829.
[28] W.E. Antholine, D.H.W. Kastrau, G.C.M. Steffens, G. Buse, W.G. Zumft, P.M.H. Kroneck, A comparative EPR investigation of the multicopper proteins nitrous-oxide reductase and cytochrome-*c*-oxidase, Eur. J. Biochem. 209 (1992) 875–881.
[29] R.B. Gennis, Multiple proton-conducting pathways in cytochrome oxidase and a proposed role for the active-site tyrosine, Biochim. Biophys. Acta 1365 (1998) 241–248.
[30] D.M. Popovic, A.A. Stuchebrukhov, Proton pumping mechanism and catalytic cycle of cytochrome *c* oxidase: Coulomb pump model with kinetic gating, FEBS Lett. 566 (2004) 126–130.
[31] A. Puustinen, M. Wikström, Proton exit from the heme-copper oxidase of *Escherichia coli*, Proc. Natl. Acad. Sci. U. S. A. 96 (1999) 35–37.
[32] H. Michel, Cytochrome *c* oxidase: catalytic cycle and mechanisms of proton pumping-A discussion, Biochemistry 38 (1999) 15129–15140.
[33] A. Kannt, C. Roy, D. Lancaster, H. Michel, The coupling of electron transfer and proton translocation: electrostatic calculations on *Paracoccus denitrificans* cytochrome *c* oxidase, Biophys. J. 74 (1998) 708–721.
[34] D.M. Popovic, A.A. Stuchebrukhov, Electrostatic study of the proton pumping mechanism in bovine heart cytochrome *c* oxidase, J. Am. Chem. Soc. 126 (2004) 1858–1871.
[35] J. Behr, P. Hellwig, M.W., H. Michel, Redox dependent changes at the heme propionates in cytochrome *c* oxidase from *paracoccus denitrificans*: direct evidence from FTIR difference spectroscopy in combination with heme propionate 13c labeling, Biochemistry 37 (1998) 7400–7406.
[36] M. Wikström, M.I. Verkhovsky, G. Hummer, Water-gated mechanism of proton translocation by cytochrome *c* oxidase, Biochim. Biophys. Acta 1604 (2003) 61–65.
[37] M.H.M. Olsson, P.K. Sharma, A. Warshel, Simulating redox coupled proton transfer in cytochrome *c* oxidase: looking for the proton bottleneck, FEBS Lett. 579 (2005) 2026–2034.
[38] P.E.M. Siegbahn, M.R.A. Blomberg, M.L. Blomberg, Theoretical study of the energetics of proton pumping and oxygen reduction in cytochrome oxidase, J. Phys. Chem., B 107 (2003) 10946–10955.
[39] L. Florens, B. Schmidt, J. McCracken, S. Ferguson-Miller, Fast deuterium access to the buried magnesium/manganese site in cytochrome *c* oxidase, Biochemistry 40 (2001) 7491–7497.
[40] S. Ferguson-Miller, L. Florens, B. Schmidt, L. Qin, J. McCracken, Search for the proton exit pathway in cytochrome *c* oxidase: the Mg/Mn site as probe, Abstracts of Papers of the American Chemical Society, vol. 220, 2000, p. 88-HYS.
[41] D.A. Mills, L. Florens, C. Hiser, J. Qian, S. Ferguson-Miller, Where is 'outside' in cytochrome *c* oxidase and how and when do protons get there? Biochim. Biophys. Acta 1458 (2000) 180–187.
[42] D.A. Mills, S. Ferguson-Miller, Proton uptake and release in cytochrome *c* oxidase: separate pathways in time and space? Biochim. Biophys. Acta, Bioenerg. 1365 (1998) 46–52.
[43] J. Qian, W.J. Shi, M. Pressler, C. Hoganson, D. Mills, G.T. Babcock, S. Ferguson-Miller, Aspartate-407 in *Rhodobacter sphaeroides* cytochrome *c* oxidase is not required for proton pumping or manganese binding, Biochemistry 36 (1997) 2539–2543.
[44] B. Schmidt, J. McCracken, S. Ferguson-Miller, A discrete water exit pathway in the membrane protein cytochrome *c* oxidase, PNAS 100 (2003) 15539–15542.
[45] J.W. Thomas, A. Puustinen, J.O. Alben, R.B. Gennis, M. Wikström, Substitution of asparagine for aspartate-135 in subunit I of the cytochrome bo ubiquinol oxidase of *Escherichia coli* eliminates proton-pumping activity, Biochemistry 32 (1993) 10923–10928.
[46] J.R. Fetter, J. Qian, J. Shapleigh, J.W. Thomas, A. García-Horsman, E. Schmidt, J. Hosler, G.T. Babcock, R.B. Gennis, S. Ferguson-Miller, Possible proton relay pathways in cytochrome *c* oxidase, Proc. Natl. Acad. Sci. U. S. A. 92 (1995) 1604–1608.
[47] J.A. García-Horsman, A. Puustinen, R.B. Gennis, M. Wikström, Proton transfer in cytochrome bo_3 ubiquinol oxidase of *Escherichia coli*: second-site mutations in subunit I that restore proton pumping in the mutant Asp135→Asn, Biochemistry 34 (1995) 4428–44233.
[48] J. Xu, G.A. Voth, Computer simulation of explicit proton translocation in cytochrome *c* oxidase: the D-pathway, Proc. Natl. Acad. Sci. U. S. A. 102 (2005) 6795–6800.
[49] R. Pomès, G. Hummer, M. Wikström, Structure and dynamics of a proton shuttle in cytochrome *c* oxidase, Biochim. Biophys. Acta 1365 (1998) 255–260.
[50] I. Hofacker, K. Schulten, Oxygen and proton pathways in cytochrome *c* oxidase, Proteins 30 (1998) 100–107.
[51] P. Ädelroth, M. Karpefors, G. Gilderson, F.L. Tomson, R.B. Gennis, P. Brzezinski, Proton transfer from glutamate 286 determines the transition rates between oxygen intermediates in cytochrome *c* oxidase, Biochim. Biophys. Acta 1459 (2000) 533–539.
[52] M. Tashiro, A.A. Stuchebrukhov, Thermodynamic properties of internal water molecules in the hydrophobic cavity around the catalytic center of cytochrome *c* oxidase, J. Phys. Chem., B 109 (2005) 1015–1022.
[53] X. Zheng, D.M. Medvedev, J. Swanson, A.A. Stuchebrukhov, Computer simulation of water in cytochrome *c* oxidase, Biochim. Biophys. Acta 1557 (2003) 99–107.
[54] S. Riistama, G. Hummer, A. Puustinen, R.B. Dyer, W.H. Woodruff, M. Wikström, Bound water in the proton translocation mechanism of the haem-copper oxidases, FEBS Lett. 414 (1997) 275–280.
[55] M. Wikström, C. Ribacka, M. Molin, L. Laakkonen, M. Verkhovsky, A. Puustinen, Gating of proton and water transfer in the respiratory enzyme cytochrome *c* oxidase, Proc. Natl. Acad. Sci. U. S. A. 102 (2005) 10478–10481.
[56] J.X. Ma, P.H. Tsatsos, D. Zaslavsky, B. Barquera, J.W. Thomas, A. Katsonouri, A. Puustinen, M. Wikström, P. Brzezinski, J.O. Alben, R.B. Gennis, Glutamate-89 in subunit II of cytochrome bo_3 from *Escherichia coli* is required for the function of the heme-copper oxidase, Biochemistry 38 (1999) 15150–15156.

[57] M. Brändén, F. Tomson, R.B. Gennis, P. Brzezinski, The entry point of the K-proton-transfer pathway in cytochrome *c* oxidase, Biochemistry 41 (2002) 10794–10798.
[58] A. Kannt, C.R. Lancaster, H. Michel, The role of electrostatic interactions for cytochrome *c* oxidase function, J. Bioenerg. Biomembranes 30 (1998) 81–87.
[59] J.P. Hosler, S. Ferguson-Miller, M.W. Calhoun, J.W. Thomas, J. Hill, L. Lemieux, J. Ma, C. Georgiou, J. Fetter, J. Shapleigh, M.M.J. Tecklenburg, G.T. Babcock, R.B. Gennis, Insight into the active-site structure and function of cytochrome oxidase by analysis of site-directed mutants of bacterial cytochrome aa_3 and cytochrome bo, J. Bioenerg. Biomembranes 25 (1993) 121–136.
[60] J.P. Hosler, J.P. Shapleigh, D.M. Mitchell, Y. Kim, M.A. Pressler, C. Georgiou, G.T. Babcock, J.O. Alben, S. Ferguson-Miller, R.B. Gennis, Polar residues in helix VIII of subunit I of cytochrome *c* oxidase influence the activity and the structure of the active site, Biochemistry 35 (1996) 10776–10783.
[61] R.I. Cukier, A molecular dynamics study of water chain formation in the proton-conducting K channel of cytochrome *c* oxidase, Biochim. Biophys. Acta 1706 (2005) 134–146.
[62] M. Brändén, H. Sigurdson, A. Namslauer, R.B. Gennis, P. Ädelroth, P. Brzezinski, On the role of the K-proton transfer pathway in cytochrome *c* oxidase, Proc. Natl. Acad. Sci. U. S. A. 98 (2001) 5013–5018.
[63] S. Yoshikawa, K. Shinzawa-Itoh, T. Tsukihara, Crystal structure of bovine heart cytochrome *c* oxidase at 2.8 A resolution, J. Bioenerg. Biomembranes 30 (1998) 7–14.
[64] T. Tsukihara, K. Shimokata, Y. Katayama, H. Shimada, K. Muramoto, H. Aoyama, M. Mochizuki, K. Shinzawa-Itoh, E. Yamashita, M. Yao, Y. Ishimura, S. Yoshikawa, The low-spin heme of cytochrome *c* oxidase as the driving element of the proton-pumping process, Proc. Natl. Acad. Sci. U. S. A. 100 (2003) 15304–15309.
[65] H.M. Lee, T.K. Das, D.L. Rousseau, D. Mills, S. Ferguson-Miller, R.B. Gennis, Mutations in the putative H-channel in the cytochrome *c* oxidase from *Rhodobacter sphaeroides* show that this channel is not important for proton conduction but reveal modulation of the properties of heme a, Biochemistry 39 (2000) 2989–2996.
[66] U. Pfitzner, A. Odenwald, T. Ostermann, L. Weingard, B. Ludwig, O.M. H. Richter, Cytochrome *c* oxidase (Heme aa(3)) from *Paracoccus denitrificans*: analysis of mutations in putative proton channels of subunit I, J. Bioenerg. Biomembranes 30 (1998) 89–97.
[67] J. Salje, B. Ludwig, O.M. Richter, Is a third proton-conducting pathway operative in bacterial cytochrome *c* oxidase? Biochem. Soc. Trans. 33 (2005) 829–831.
[68] G.T. Babcock, How oxygen is activated and reduced in respiration, Proc. Natl. Acad. Sci. U. S. A. 96 (1999) 12971–12973.
[69] M.R.A. Blomberg, P.E.M. Siegbahn, G.T. Babcock, M. Wikström, O – O bond splitting mechanism in cytochrome oxidase, J. Inorg. Biochem. 80 (2000) 261–269.
[70] M. Wikström, M.I. Verkhovsky, Proton translocation by cytochrome *c* oxidase in different phases of the catalytic cycle, Biochim. Biophys. Acta, Bioenerg. 1555 (2002) 128–132.
[71] D. Bloch, I. Belevich, A. Jasaitis, C. Ribacka, A. Puustinen, M.I. Verkhovsky, M. Wikström, The catalytic cycle of cytochrome *c* oxidase is not the sum of its two halves, Proc. Natl. Acad. Sci. U. S. A. 101 (2004) 529–533.
[72] M. Wikström, Cytochrome *c* oxidase: 25 years of the elusive proton pump, Biochim. Biophys. Acta 1655 (2004) 241–247.
[73] M.I. Verkhovsky, A. Tuukkanen, C. Backgren, A. Puustinen, M. Wikström, Charge translocation coupled to electron injection into oxidized cytochrome *c* oxidase from *Paracoccus denitrificans*, Biochemistry 40 (2001) 7077–7083.
[74] Ó. Einarsdóttir, I. Szundi, Time-resolved optical absorption studies of cytochrome oxidase dynamics, Biochim. Biophys. Acta, Bioenerg. 1655 (2004) 263–273.
[75] P. Ädelroth, in: M.W. Ed (Ed.), Biophysical and Structural Aspects of Bioenergetics, Royal Society of Chemistry, Cambridge, UK, 2005, pp. 72–98.
[76] J.E. Morgan, M.I. Verkhovsky, M. Wikström, Observation and assignment of peroxy and ferryl intermediates in the reduction of dioxygen to water by cytochrome *c* oxidase, Biochemistry 35 (1996) 12235–12240.
[77] Ó. Einarsdóttir, I. Szundi, N. Van Eps, A. Sucheta, P(M) and P(R) forms of cytochrome *c* oxidase have different spectral properties, J. Inorg. Biochem. 91 (2002) 87–93.
[78] K. Faxén, G. Gilderson, P. Ädelroth, P. Brzezinski, A mechanistic principle for proton pumping by cytochrome *c* oxidase, Nature 437 (2005) 286–289.
[79] D. Zaslavsky, A.D. Kaulen, I.A. Smirnova, T. Vygodina, A.A. Konstantinov, Flash-induced membrane potential generation by cytochrome *c* oxidase, FEBS Lett. 336 (1993) 389–393.
[80] M.I. Verkhovsky, J.E. Morgan, M.L. Verkhovskaya, M. Wikström, Translocation of electrical charge during a single turnover of cytochrome-*c* oxidase, Biochim. Biophys. Acta 1318 (1997) 6–10.
[81] P. Ädelroth, M. Ek, P. Brzezinski, Factors determining electron-transfer rates in cytochrome *c* oxidase: investigation of the oxygen reaction in the *R. sphaeroides* and bovine enzymes, Biochim. Biophys. Acta 1367 (1998) 107–117.
[82] P. Ädelroth, M. Svensson Ek, D.M. Mitchell, R.B. Gennis, P. Brzezinski, Glutamate 286 in cytochrome aa3 from *Rhodobacter sphaeroides* is involved in proton uptake during the reaction of the fully-reduced enzyme with dioxygen, Biochemistry 36 (1997) 13824–13829.
[83] P. Brzezinski, P. Ädelroth, Pathways of proton transfer in cytochrome *c* oxidase, J. Bioenerg. Biomembranes 30 (1998) 99–107.
[84] A.A. Konstantinov, S. Siletsky, D. Mitchell, A. Kaulen, R.B. Gennis, The roles of the two proton input channels in cytochrome *c* oxidase from *Rhodobacter sphaeroides* probed by the effects of site-directed mutations on time-resolved electrogenic intraprotein proton transfer, Proc. Natl. Acad. Sci. U. S. A. 94 (1997) 9085–9090.
[85] T.V. Vygodina, C. Pecoraro, D. Mitchell, R. Gennis, A.A. Konstantinov, Mechanism of inhibition of electron transfer by amino acid replacement K362M in a proton channel of *Rhodobacter sphaeroides* cytochrome *c* oxidase, Biochemistry 37 (1998) 3053–3061.
[86] M. Ruitenberg, A. Kannt, E. Bamberg, B. Ludwig, H. Michel, K. Fendler, Single-electron reduction of the oxidized state is coupled to proton uptake via the K pathway in *Paracoccus denitrificans* cytochrome *c* oxidase, Proc. Natl. Acad. Sci. U. S. A. 97 (2000) 4632–4636.
[87] M. Wikström, A. Jasaitis, C. Backgren, A. Puustinen, M.I. Verkhovsky, The role of the D- and K-pathways of proton transfer in the function of the haem-copper oxidases, Biochim. Biophys. Acta 1459 (2000) 514–520.
[88] M. Karpefors, P. Ädelroth, A. Aagaard, I.A. Smirnova, P. Brzezinski, The deuterium isotope effect as a tool to investigate enzyme catalysis: proton-transfer control mechanisms in cytochrome *c* oxidase, Isr. J. Chem. 39 (1999) 427–437.
[89] M. Karpefors, P. Ädelroth, P. Brzezinski, Localized control of proton transfer through the D-pathway in cytochrome *c* oxidase: application of the proton-inventory technique, Biochemistry 39 (2000) 6850–6856.
[90] Y. Marantz, E. Nachliel, A. Aagaard, P. Brzezinski, M. Gutman, The proton collecting function of the inner surface of cytochrome *c* oxidase from *Rhodobacter sphaeroides*, Proc. Natl. Acad. Sci. U. S. A. 95 (1998) 8590–8595.
[91] S. Checover, E. Nachliel, N.A. Dencher, M. Gutman, Mechanism of proton entry into the cytoplasmic section of the proton-conducting channel of bacteriorhodopsin, Biochemistry 36 (1997) 13919–13928.
[92] Y. Marantz, O. Einarsdóttir, E. Nachliel, M. Gutman, Proton-collecting properties of bovine heart cytochrome *c* oxidase: kinetic and electrostatic analysis, Biochemistry 40 (2001) 15086–15097.
[93] L. Salomonsson, K. Faxén, P. Ädelroth, P. Brzezinski, The timing of proton migration in membrane-reconstituted cytochrome *c* oxidase, Proc. Natl. Acad. Sci. U. S. A. 102 (2005) 17624–17629.
[94] C. Ribacka, M.I. Verkhovsky, I. Belevich, D.A. Bloch, A. Puustinen, M. Wikström, An elementary reaction step of the proton pump is revealed by mutation of tryptophan-164 to phenylalanine in cytochrome *c* oxidase from *Paracoccus denitrificans*, Biochemistry 44 (2005) 16502–16512.
[95] G. Brändén, M. Brändén, B. Schmidt, D.A. Mills, S. Ferguson-Miller, P. Brzezinski, The protonation state of a heme propionate controls

electron transfer in cytochrome *c* oxidase, Biochemistry 44 (2005) 10466–10474.
[96] M. Oliveberg, P. Brzezinski, B.G. Malmström, The effect of pH and temperature on the reaction of fully reduced and mixed-valence cytochrome *c* oxidase with dioxygen, Biochim. Biophys. Acta 977 (1989) 322–328.
[97] Y.J. Zhen, B. Schmidt, U.G. Kang, W. Antholine, S. Ferguson-Miller, Mutants of the Cu-A site in cytochrome *c* oxidase of *Rhodobacter sphaeroides*: I. Spectral and functional properties, Biochemistry 41 (2002) 2288–2297.
[98] M. Karpefors, P. Ädelroth, Y. Zhen, S. Ferguson-Miller, P. Brzezinski, Proton uptake controls electron transfer in cytochrome *c* oxidase, Proc. Natl. Acad. Sci. U. S. A. 95 (1998) 13606–13611.
[99] D. Zaslavsky, R.C. Sadoski, K.F. Wang, B. Durham, R.B. Gennis, F. Millett, Single electron reduction of cytochrome *c* oxidase compound F: resolution of partial steps by transient spectroscopy, Biochemistry 37 (1998) 14910–14916.
[100] I.A. Smirnova, P. Ädelroth, R.B. Gennis, P. Brzezinski, Aspartate-132 in cytochrome *c* oxidase from *Rhodobacter sphaeroides* is involved in a two-step proton transfer during oxo-ferryl formation, Biochemistry 38 (1999) 6826–6833.
[101] D. Zaslavsky, R.B. Gennis, R.C. Sadoski, S. Rajagukguk, L. Geren, F. Millett, B. Durham, Direct measurement of proton release by cytochrome *c* oxidase in solution during the F?O transition, Proc. Natl. Acad. Sci. U. S. A. 101 (2004) 10544–10547.
[102] R.C. Sadoski, D. Zaslavsky, R.B. Gennis, B. Durham, F. Millett, Exposure of bovine cytochrome *c* oxidase to high triton X-100 or to alkaline conditions causes a dramatic change in the rate of reduction of compound F, J. Biol. Chem. 276 (2001) 33616–33620.
[103] D.L. Zaslavsky, I.A. Smirnova, S.A. Siletsky, A.D. Kaulen, F. Millett, A.A. Konstantinov, Rapid kinetics of membrane potential generation by cytochrome *c* oxidase with the photoactive Ru(II)-tris-bipyridyl derivative of cytochrome *c* as electron donor, FEBS Lett. 359 (1995) 27–30.
[104] S.A. Siletsky, A.S. Pawate, K. Weiss, R.B. Gennis, A.A. Konstantinov, Transmembrane charge separation during the ferryl-oxo → oxidized transition in a nonpumping mutant of cytochrome *c* oxidase, J. Biol. Chem. 279 (2004) 52558–52565.
[105] A. Namslauer, A. Aagaard, A. Katsonouri, P. Brzezinski, Intramolecular proton-transfer reactions in a membrane-bound proton pump: the effect of pH on the peroxy to ferryl transition in cytochrome *c* oxidase, Biochemsitry 42 (2003) 1488–1498.
[106] G. Gilderson, L. Salomonsson, A. Aagaard, J. Gray, P. Brzezinski, J. Hosler, Subunit III of cytochrome *c* oxidase of *Rhodobacter sphaeroides* is required to maintain rapid proton uptake through the D pathway at physiologic pH, Biochemistry 42 (2003) 7400–7409.
[107] P. Ädelroth, P. Brzezinski, B.G. Malmström, Internal electron transfer in cytochrome *c* oxidase from *Rhodobacter sphaeroides*, Biochemistry 34 (1995) 2844–2849.
[108] A.J. Moody, 'As prepared' forms of fully oxidised haem/Cu terminal oxidases, Biochim. Biophys. Acta 1276 (1996) 6–20.
[109] E. Antonini, M. Brunori, A. Colosimo, C. Greenwood, M.T. Wilson, Oxygen "pulsed" cytochrome *c* oxidase: functional properties and catalytic relevance, Proc. Natl. Acad. Sci. U. S. A. 74 (1977) 3128–3132.
[110] M. Ruitenberg, A. Kannt, E. Bamberg, K. Fendler, H. Michel, Reduction of cytochrome *c* oxidase by a second electron leads to proton translocation, Nature 417 (2002) 99–102.
[111] P. Brzezinski, Redox-driven membrane-bound proton pumps, Trends Biochem. Sci. 29 (2004) 380–387.
[112] F. Garczarek, K. Gerwert, Functional waters in intraprotein proton transfer monitored by FTIR difference spectroscopy, Nature 439 (2006) 109–112.